Human Molecular Genetics, 2012, Vol. 21, No. 23 ***5131–5146***
doi:10.1093/hmg/dds360
Advance Access published on August 27, 2012

Abnormal interaction of VDAC1 with amyloid beta and phosphorylated tau causes mitochondrial dysfunction in Alzheimer's disease

Maria Manczak[1] and P. Hemachandra Reddy[1,2,*]

[1]Neurogenetics Laboratory, Division of Neuroscience, Oregon National Primate Research Center, Oregon Health and Science University, 505 NW 185th Avenue, Beaverton, OR 97006, USA and [2]Department of Physiology and Pharmacology, Oregon Health and Science University, 3181 SW Sam Jackson Park Road, Portland, OR 97239, USA

Received July 20, 2012; Revised and Accepted August 21, 2012

The purpose of our study was to determine the relationship between voltage-dependent anion channel 1 protein (VDAC1) and amyloid beta (Aβ) and phosphorylated tau in Alzheimer's disease (AD). Using brain specimens from AD patients, control subjects and 6-, 12- and 24-month-old Aβ precursor protein (APP) transgenic mice, we studied VDAC1 protein levels. Further, we also studied the interaction between VDAC1 and Aβ (monomers and oligomers) and phosphorylated tau, using cortical issues from AD patients, control subjects, APP, APP/PS1 and 3XTg.AD mice. We also studied age- and VDAC1-linked, mutant APP/Aβ-induced mitochondrial dysfunction in APP and non-transgenic wild-type (WT) mice. We found progressively increased levels of VDAC1 in the cortical tissues from the brains of patients with AD, relative to control subjects, and significantly increased levels of VDAC1 in the cerebral cortices of 6-, 12- and 24-month-old APP transgenic mice, relative to the age-matched control WT mice. Interestingly, we found VDAC1 interacted with Aβ and phosphorylated tau in the brains from AD patients and from APP, APP/PS1 and 3XTg.AD mice. We found progressively increased mitochondrial dysfunction in APP mice relative to WT mice. These observations led us to conclude that VDAC1 interacts with Aβ, and phosphorylated tau may in turn block mitochondrial pores, leading to mitochondrial dysfunction in AD pathogenesis. Based on current study observations, we propose that reduced levels of VDAC1, Aβ and phosphorylated tau may reduce the abnormal interaction between VDAC1 and APP, VDAC1 and Aβ, and VDAC1 and phosphorylated tau; and that reduced levels of VDAC1, Aβ and phosphorylated tau may maintain normal mitochondrial pore opening and pore closure, ultimately leading to normal mitochondrial function, mitochondria supplying ATP to nerve terminals and boosting synaptic and cognitive function in AD.

INTRODUCTION

Alzheimer's disease (AD) is a progressive, age-dependent neurodegenerative disorder, characterized clinically by the impairment of cognitive functions and changes in behavior and personality (1–4). AD is associated with intracellular neurofibrillary tangles and extracellular amyloid beta (Aβ) plaques in regions of the brain that are responsible for learning and memory. In addition, AD is also associated with synaptic damage, abnormal mitochondrial structural and functional alterations and the proliferation of reactive astrocytes and microglia (2,3,5–7). Among these cellular changes, mitochondrial oxidative damage and synaptic dysfunction have been reported as early events in AD pathogenesis (4,8). However, the causal factors of mitochondrial dysfunction and synaptic pathology in AD pathogenesis are not well understood. Further, the precise link between Aβ/hyperphosphorylated tau and the structure/function of mitochondria in the development and progression of AD is also not well understood.

Mitochondrial dysfunction has been identified in AD postmortem brains (9–14), APP transgenic mice (15–23), cells that express mutant Aβ precursor protein (APP) and cells treated with Aβ (17,24–32). Several studies found increased free radical production, lipid peroxidation, oxidative DNA and

*To whom correspondence should be addressed. Tel: +1 5034182625; Fax: +1 5034182701; Email: reddyh@ohsu.edu

protein damage and reduced ATP production in brains from AD patients, compared with control subjects (10,12–14,33–35). The mechanistic link between mitochondria and AD pathogenesis has only recently been confirmed. Using biochemical, molecular and electron microscopy studies, and AD postmortem brains and brains from AβPP mice, we (16,25) and others (18–20,36,37) found that Aβ is associated with mitochondrial dysfunction and is responsible for increasing free radicals. Further, recently Yan and colleagues (38) reported that Aβ interacts with mitochondrial matrix proteins, alcohol-induced Aβ dehydrogenase (ABAD) (21) and cyclophilin D (CypD). The abnormal interactions between Aβ and matrix proteins ABAD and CypD induce elevated free radicals and cause mitochondrial dysfunction in AD neurons (21,38). However, the mechanistic link between Aβ and mitochondrial damage is not well understood.

In AD brains, hyperphosphorylated tau and neurofibrillary tangles have been extensively reported as a second major pathological hallmark (39), and increasing evidence suggests that hyperphosphorylated tau is involved in mitochondrial dysfunction and neuronal damage. Several studies reported that mutant tau is capable of reducing anterograde transport of vesicles and cell organelles by blocking microtubule tracks (40–43). Using murine primary neurons, Vossel *et al.* (44) studied the effects of tau and Aβ on mitochondrial axonal transport and the neurotrophin factor TrkA. They found that Aβ oligomers inhibited mitochondrial axonal transport in wild-type (WT) primary neurons, but neurons that expressed reduced tau showed normal axonal mitochondrial transport, suggesting that: (i) Aβ may require tau phosphorylation in order for Aβ to impair axonal transport and (ii) a reduction in tau may protect against Aβ-induced axonal transport changes in AD neurons (44). Further, several research groups found mitochondrial functional defects in 3xTg.AD transgenic mice (19,45,46), and in P301L, P301S and PS2/Tau transgenic mice (47–50), other researchers found deregulated mitochondrial proteins, particularly complexes I and IV of oxidative phosphorylation, and increased free radicals and lipid peroxidation (47–50).

Mitochondria are cytoplasmic organelles that are essential for the life and death of cells. They perform several cellular functions, including the regulation of intracellular calcium, ATP production, free radical production and scavenging and the release of proteins that activate the caspase family of proteases (51). Mitochondria are compartmentalized into two lipid membranes: the inner membrane and the outer membrane. The inner membrane houses the mitochondrial respiratory chain and provides a highly efficient barrier to ionic flow. It also covers the mitochondrial matrix, which contains the components of tricarboxylic acid cycle and beta oxidation (51). The outer membrane is highly porous, allowing low-molecular-weight substances between the cytosol and the intermembrane space. Oxidative phosphorylation requires the transport of metabolites, including ADP, ATP and inorganic phosphorous (Pi) across the mitochondrial membranes and cytoplasm. Voltage-dependent anion channel proteins (VDACs), which are ubiquitously located in the mitochondrial outer membrane, are generally thought to be the primary means by which metabolites diffuse in and out of mitochondria (52–55). Three VDAC isoforms (VDAC1, VDAC2 and VDAC3) have been found in mammalian mitochondria, with VDAC1 and VDAC3 shown to have 9 exons and VDAC2, 10 exons. The additional exon in VDAC2 is believed to encode part of the 5′-UTR region (56,57). Of the three VDAC isoforms, VDAC1 is the most widely expressed isoform, followed by VDAC2 and then VDAC3 (58,59). VDAC1 and VDAC2 are expressed in the heart, liver and skeletal muscles and in the brain. Interestingly, VDAC1 is expressed in very low levels in the testes, and VDAC2 is expressed in high levels in the same tissues (56,57). VDAC3 is expressed in testes, liver, ovary, adrenal, lung, spleen and kidney muscles (60).

VDACs perform several important functions in the cell, including regulating cell survival and growth; maintaining synaptic plasticity through mitochondrial permeability in the transition pore, mitochondrial shape and structural change; regulating hexokinase interactions with mitochondria; and regulating apoptosis signaling (61,62). Changes in mitochondrial permeability occur when apoptosis is mediated by the Bcl-2 family of proteins which bind to VDAC1 and alter channel kinetics and conductance. Homodimerization of VDAC may be a mechanism for changing mitochondrial permeability and supporting the release of cytochrome *c* (63). Recent research also revealed that VDAC channel is inhibited by the cytoskeletal protein tubulin and causes impairments in channel conductance (64). In addition, several recent studies revealed that VDAC proteins and their binding partners are modified post-translationally due to VDAC1 hyperphosphorylation and that phosphorylated VDAC1 is involved in the malfunction of VDAC1 (65,66). However, the VDAC1 link to mutant AD proteins, such as Aβ and phosphorylated tau, is as yet unexplored.

In the current study, we sought to determine: (i) age-dependent, altered VDAC1 protein levels in AD brains and mice that express mutant APP and (ii) Aβ and phosphorylated tau physical interaction with VDAC proteins in AD brains, APP, APP/PS1 and 3XTg.AD mice, and (iii) age-dependent, VDAC1-mediated and Aβ-induced oxidative stress and mitochondrial dysfunction in a well-characterized APP transgenic mice (Tg2576 line).

RESULTS

VDAC1 protein levels in AD brains

Using immunoblotting analysis and quantitative densitometry, we quantified VDAC1 in frontal cortical tissues from patients at different stages of AD progression to determine whether VDAC1 is altered as AD progresses (Fig. 1). Our immunoblotting findings of VDAC1 agreed with our previously published real-time RT–PCR findings (17). VDAC1 levels were significantly increased in AD patients at Braak stages I and II ($P = 0.003$), III and IV ($P = 0.001$) and V and VI ($P = 0.001$), compared with the corresponding VDAC1 levels in control subjects. These findings suggest that VDAC1 levels progressively increase as AD progresses.

Age-dependent VDAC1 protein levels in APP and non-transgenic WT mice

Using immunoblotting analysis and quantitative densitometry, we quantified VDAC1 protein levels in cerebral cortex tissues

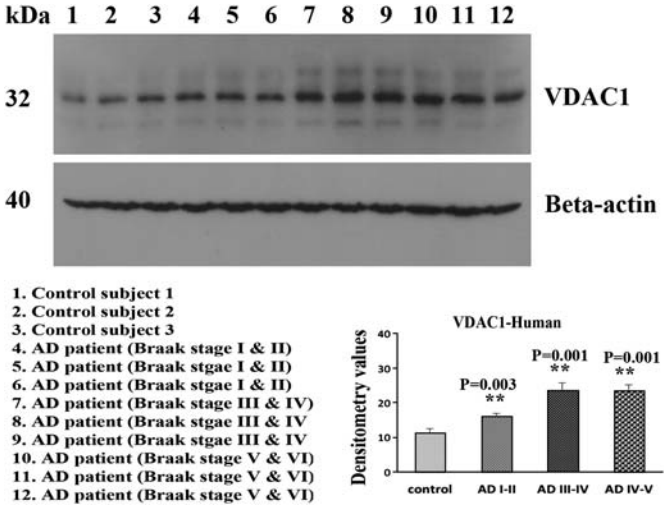

Figure 1. Representative immunoblots of VDAC1 in brains from AD patients and control subjects. VDAC1 levels were significantly higher in AD patients at Braak stages I and II ($P = 0.003$), III and IV ($P = 0.001$) and V and VI ($P = 0.001$), compared with VDAC1 in control subjects.

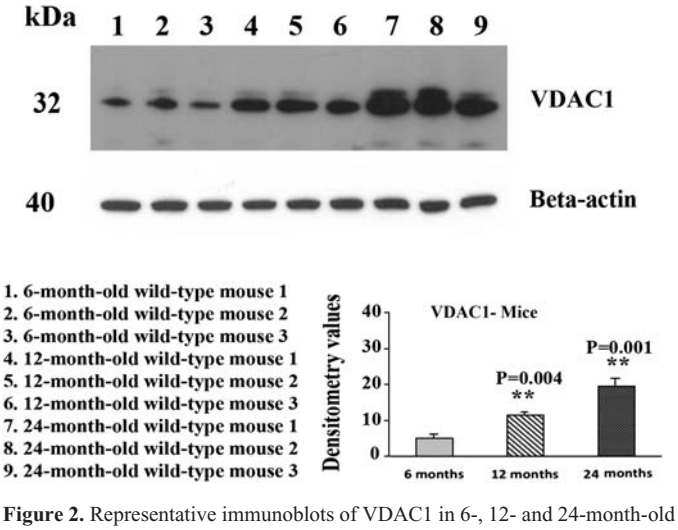

Figure 2. Representative immunoblots of VDAC1 in 6-, 12- and 24-month-old non-transgenic WT mice. VDAC1 levels were significantly higher in the 12-month-old ($P = 0.004$) and 24-month-old WT mice ($P = 0.001$), compared with VDAC1 in the 6-month-old WT mice.

from 6-, 12- and 24-month APP mice and age-matched non-transgenic WT mice in order to determine whether VDAC1 increases with age in Aβ-overexpressed APP transgenic mice. As shown in Figure 2, we found significantly increased levels of VDAC1 in 12-month-old ($P = 0.004$) and 24-month-old ($P = 0.001$) non-transgenic WT mice, relative to 6-month-old WT mice, indicating an age-dependent increase in VDAC1, in the cerebral cortex of the WT mice. To determine whether age-dependent mutant APP and/or Aβ elevates VDAC1, we also analyzed VDAC1 immunoblotting data in 6-, 12- and 24-month-old APP mice. As shown in Figure 3, we found significantly increased levels of VDAC1 in 12-month-old ($P = 0.01$) and 24-month-old ($P = 0.001$) APP mice, relative to 6-month-old APP mice, indicating an age-dependent increase of VDAC1 in the cerebral cortex of APP mice. To determine whether mutant APP and/or Aβ elevates VDAC1, we also compared VDAC1 immunoblotting and densitometry data with age-matched WT mice immunoblotting and densitometry data. We found significantly increased levels of VDAC1 in 6-month-old ($P = 0.003$) and 12-month-old ($P = 0.01$) APP mice, relative to the 6- and 12-month-old non-transgenic WT mice (Fig. 3). However, we did not find any marked differences in the levels of VDAC1 in the 24-month-old APP mice, relative to age-matched WT mice.

VDAC1 interaction with Aβ

To determine whether Aβ monomers and/or oligomers interact with VDAC1, we conducted immunoprecipitation analysis, using cortical protein lysates from brains of AD patients (Braak stages III and IV, and V and VI) and of control subjects (Braak stage 0) and from brains of 20-month-old APP and APP/PS1 transgenic mice and of age-matched WT mice, and antibodies of Aβ (6E10 monoclonal A11 oligomeric Aβ) and VDAC1 (see Table 1 for details). Our immunoprecipitation and immunoblotting analyses using VDAC1 antibody (Bioss, MA, USA) revealed a 32 kDa VDAC1 band and a 60 kDa phosphorylated VDAC1 band in the immunoprecipitation elutes from control subject and AD patient, and from WT mouse and 20-month-old APP mouse, suggesting that VDAC antibody that we used for immunoprecipitation is specific for VDAC1 (Fig. 4A).

We next studied VDAC1 interaction with Aβ in cortical protein lysates from AD patients and control subjects and 20-month-old APP and APP/PS1 mice and WT mice. Our immunoprecipitation analysis with VDAC1 antibody and immunoblotting with the Aβ antibody (6E10) revealed a 4 kDa Aβ and 100 kDa full-length APP in VDAC1 immunoprecipitation elutes from definite and severe AD patients and from 20-month-old APP and APP/PS1 mice (Fig. 4A). However, in control subjects and 20-month-old non-transgenic WT mice, we found no interaction between VDAC1 and Aβ (monomeric Aβ) and between VDAC1 and full-length APP. Similar to monomeric Aβ, we also found oligomeric Aβ in VDAC1 immunoprecipitation elutes from definite and severe AD patients and from 20-month-old APP and APP/PS1 mice (Fig. 4B).

VDAC1 interaction with phosphorylated tau

To determine whether phosphorylated tau interacts with VDAC1, we conducted immunoprecipitation analysis, using cortical protein lysates from the brains of AD patients (Braak stages I and II, III and IV, and V and VI) and of control subjects (Braak stage 0), and of 13-month-old APP, APP/PS1, 3xTg.AD transgenic mice and age-matched WT mice and antibodies of phosphorylated tau and VDAC1 (see Table 1 for details). As shown in Figure 5, our immunoprecipitation and immunoblotting analyses using phosphorylated tau antibody revealed a 60 kDa band in the immunoprecipitation elutes from the brains of AD patients (lanes 2–4) and of the 13-month-old APP (lane 6), APP/PS1 (lane 7) and 3xTg.AD mice (lane 8). However, we did not find any band in the protein lysates of the control subjects (lane1) and of the 13-month-old non-transgenic WT mice (lane 5A),

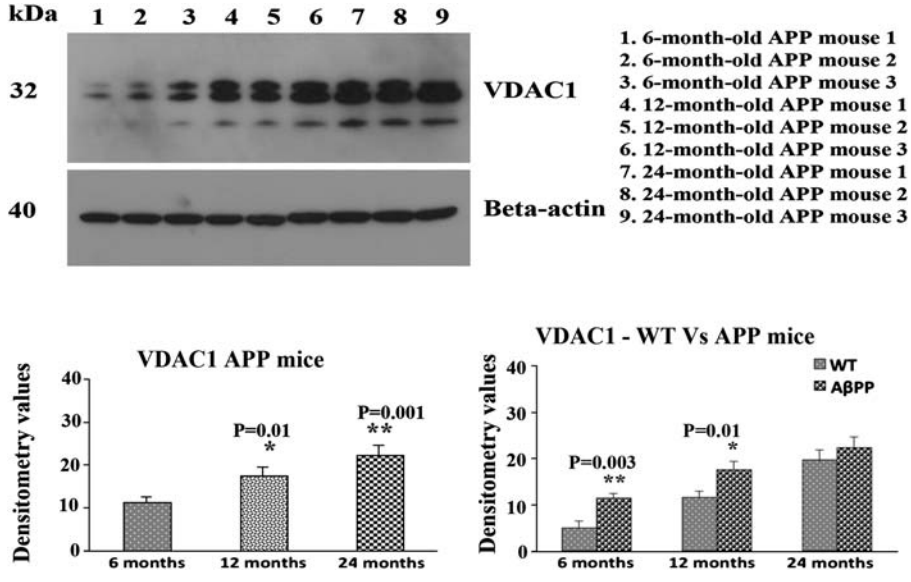

Figure 3. Representative immunoblots of VDAC1 in 6-, 12- and 24-month-old APP mice. VDAC1 levels were significantly higher in 12-month-old ($P = 0.01$) and 24-month-old WT mice ($P = 0.001$), compared with VDAC1 in the 6-month-old APP mice. VDAC1 levels were significantly higher in 6-month-old ($P = 0.003$) and 12-month-old APP mice ($P = 0.01$), compared with VDAC1 in 6- and 12-month-old WT mice.

Table 1. Summary of antibody dilutions and conditions used in the co-immunoprecipitation

Marker	Primary antibody (species and dilution)	Purchased from (company, state)	Secondary antibody, dilution, Alexa dye	Purchased from (company, city and state)
Co-IP VDAC	Rabbit polyclonal, 10 μg/500 μg protein	Bioss USA antibody, Woburn, MA	Not applicable	Not applicable
Co-IP Tau	Mouse monoclonal, 10 μg/500 μg protein	Thermo Scientific, Rockford, IL	Not applicable	Not applicable
WB VDAC	Mouse monoclonal, 1:400	Abcam	Sheep anti-mouse, HRP, 1:8000	GE Healthcare Amersham, Piscataway, NJ
WB VDAC	Rabbit polyclonal, 1:400	Bioss USA antibody, Woburn, MA	Donkey anti-rabbit, HRP, 1:10 000	GE Healthcare Amersham, Piscataway, NJ
WB 6E10	Mouse monoclonal, 1:400	Covance, San Diego, CA	Sheep anti-mouse, HRP, 1:8000	GE Healthcare Amersham, Piscataway, NJ
WB A11	Rabbit polyclonal, 1:400	Invitrogen, Camarillo, CA	Donkey anti-rabbit, HRP, 1:10 000	GE Healthcare Amersham, Piscataway, NJ

indicating that the tau antibody involved in immunoprecipitation is specific for phosphorylated tau.

Our immunoprecipitation analysis with the phosphorylated tau antibody and immunoblotting with the VDAC1 antibody revealed a 32 kDa band in the phosphorylated tau immunoprecipitation elutes in the brains from AD patients (Braak stages I and II, III and IV, and V and VI) and from 13-month-old APP/PS1, 3xTg.AD transgenic mice (Fig. 5B). However, we also noticed that a faint band in the phosphorylated tau immunoprecipitation elutes from control subjects and non-transgenic WT mice. We also cross-checked our immunoprecipitation results, using the VDAC1 antibody for immunoprecipitation and phosphorylated tau antibody for immunoblotting. As shown in Figure 5C, we found the 60 kDa phosphorylated tau protein in the VDAC1-immunoprecipitation elutes in the brains from AD patients (Braak stages I and II, III and IV, and V and VI) and from 13-month-old APP/PS1, 3xTg.AD transgenic mice. These findings suggest that phosphorylated tau interacts with VDAC1.

Double-labeling analysis of VDAC1 and of full-length APP and Aβ in AD brains

To determine whether VDAC1 localizes and interacts with Aβ, we conducted double-labeling analysis of VDAC1 and Aβ, using specimens from the frontal cortex sections of AD patients. As shown in Figure 6, the immunoreactivity of VDAC1 was colocalized with full-length APP and Aβ, indicating that VDAC1 interacts with both full-length APP and Aβ.

To determine whether oligomeric Aβ interacts with VDAC1, we performed double-labeling analysis of VDAC1 and the A11 oligomeric-specific Aβ antibody, using specimens from the frontal cortex sections of AD patients. We found oligomeric Aβ colocalized with VDAC1 in these sections (Fig. 7). These observations agreed with our immunoprecipitation findings of VDAC1 and full-length APP, and monomeric and oligomeric Aβ (Fig. 4A and B).

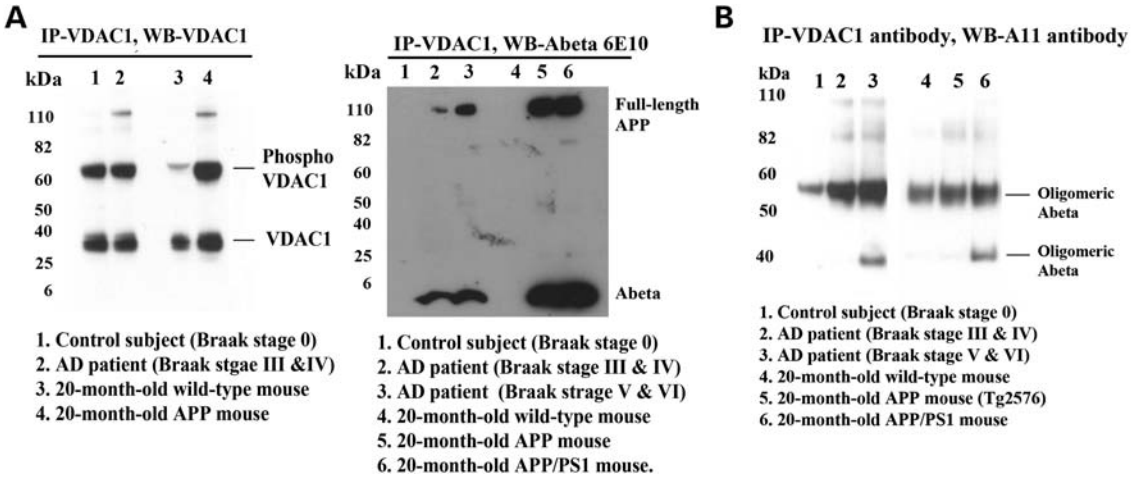

Figure 4. The specificity VDAC1 antibody for immunoprecipitation and co-immunoprecipitation analysis of VDAC1, Aβ and full-length APP in brains from patients with AD and from APP and APP/PS1 mice. (**A**) Immunoprecipitation with the VDAC1 antibody (polyclonal) and immunoblotting with the VDAC1 antibody. Immunoprecipitation with the VDAC1 antibody (polyclonal) and immunoblotting with the Aβ antibody (6E10). The 6E10 antibody immunoreacted with full-length APP and a 4 kDa Aβ in patients with definite (Braak stages III and IV) and severe (Braak stages V and VI) AD and in 20-month-old APP and APP/PS1 mice. (**B**) Immunoprecipitation with the VDAC1 antibody and immunoblotting with the oligomeric-specific A11 antibody. The A11 antibody immunoreacted with oligomeric Aβ in VDAC1 immunoprecipitation elutes in patients with definite (Braak stages III and IV) and severe (Braak stages V and VI) AD and in 20-month-old APP and APP/PS1 mice.

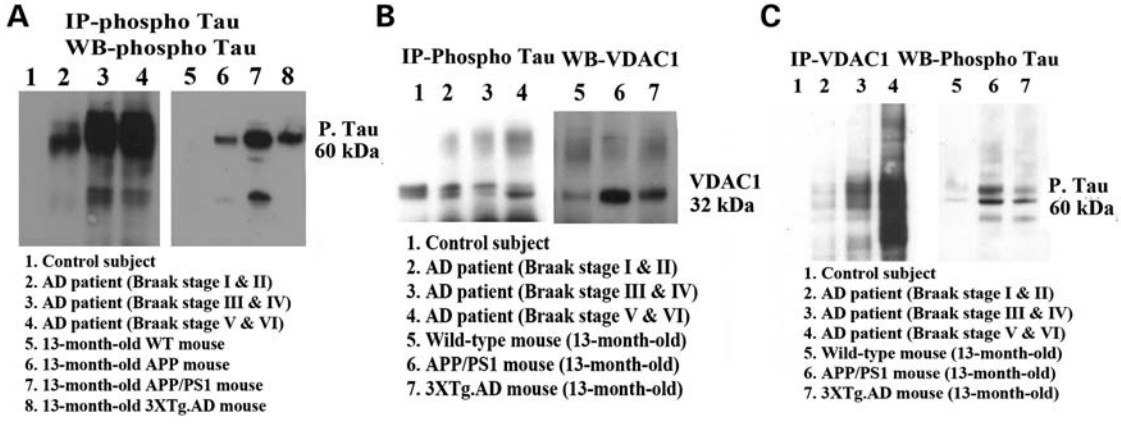

Figure 5. Co-immunoprecipitation analysis of VDAC1 and phosphorylated tau in brain tissues from AD patients and APP/PS1 and 3XTg.AD mice. (**A**) Immunoprecipitation and immunoblotting with phosphorylated tau, demonstrating that the used antibody is specific to phosphorylated tau. (**B**) Immunoprecipitation with the VDAC1 antibody and immunoblotting with phosphorylated tau, demonstrating the presence of phosphorylated tau in immunoprecipitation elutes of VDAC1. (**C**) Immunoprecipitation with the phosphorylated tau antibody and immunoblotting with the VDAC1 antibody cross-checked the interaction of VDAC1 with phosphorylated tau.

Double-labeling analysis of VDAC1 and of full-length APP and Aβ in APP mice

Using brain sections from 13-month-old APP mice, we also conducted double-labeling analysis of VDAC1 and full-length APP and Aβ in order to determine whether VDAC1 colocalizes with full-length APP and Aβ. As shown in Figure 8, the immunoreactivity of VDAC1 was colocalized with full-length APP and Aβ in the brain sections from the APP mice, further indicating that VDAC1 interacts with both full-length APP and Aβ.

Double-labeling immunofluorescence analysis of VDAC1 and of phosphorylated tau in AD brains

To determine whether VDAC1 localizes and interacts with phosphorylated tau, we conducted double-labeling analysis of VDAC1 and phosphorylated tau, using tissues from frontal cortex sections of AD patients. As shown in Figure 9, VDAC1 was colocalized with phosphorylated tau, indicating that VDAC1 interacts with phosphorylated tau. These observations matched our immunoprecipitation findings of VDAC1 and phosphorylated tau (Fig. 5).

Double-labeling immunofluorescence analysis of VDAC1 and of phosphorylated tau in 3XTg.AD mice

To determine whether VDAC1 localizes and interacts with phosphorylated tau, we conducted double-labeling analysis of VDAC1 and phosphorylated tau in tissues from the cortex and hippocampal sections of 3XTg.AD mice. As shown in Figure 9, VDAC1 immunoreactivity was colocalized with

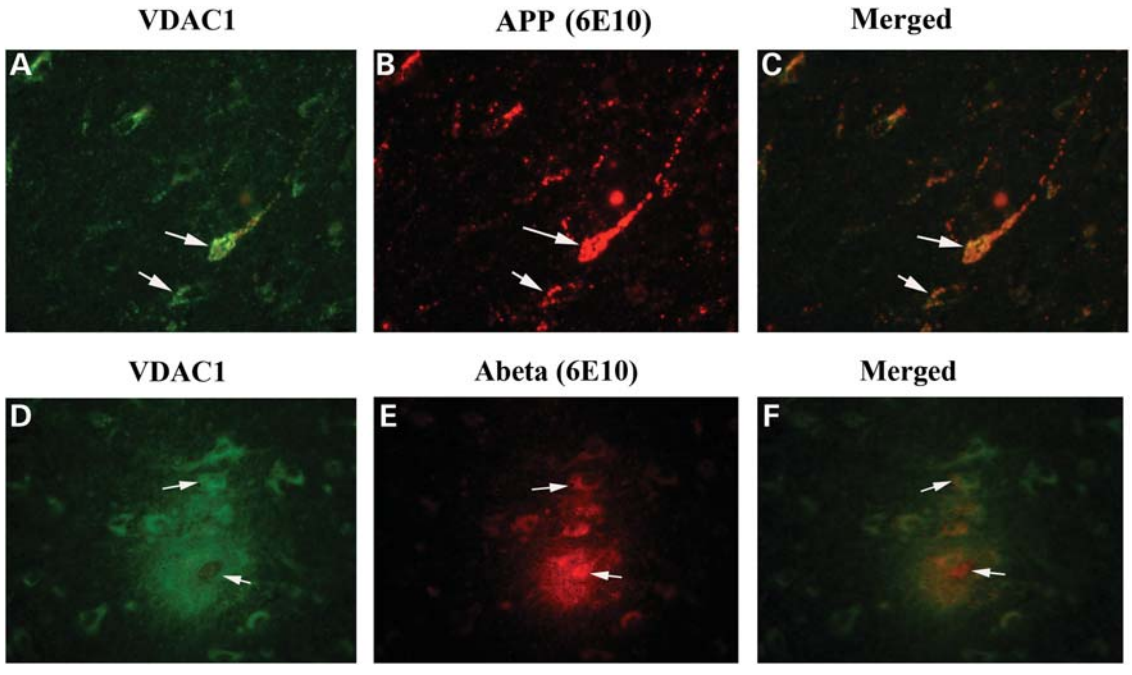

Figure 6. Double-labeling immunofluorescence analysis of VDAC1, Aβ and full-length APP in cortical sections from AD patients. The localization of VDAC1 (**A**) and APP (**B**) and the colocalization of VDAC1 and APP (merged **C**) at 40× original magnification; the localization of VDAC1 (**D**); Aβ deposits (**E**); and the colocalization of VDAC1 and Aβ deposits (merged **F**) at 100× original magnification.

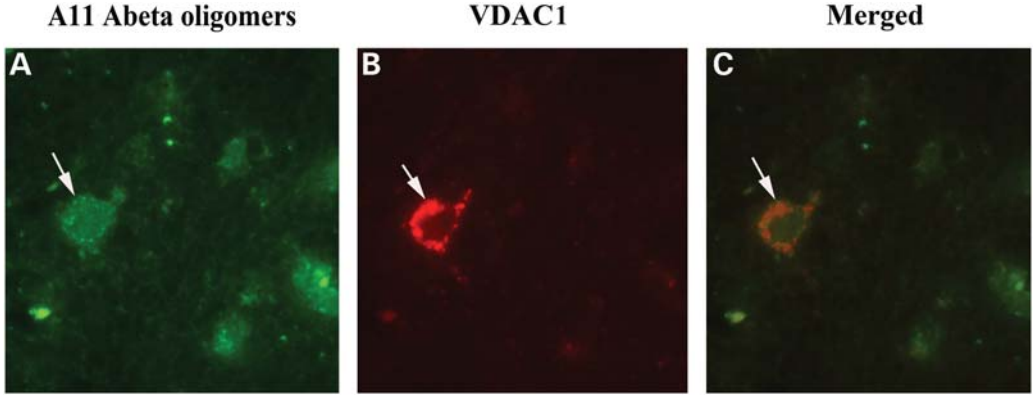

Figure 7. Double-labeling immunofluorescence analysis of VDAC1 and oligomeric Aβ in cortical sections from AD patients. The localization of VDAC1 (**A**) and oligomeric Aβ (**B**) and the colocalization of VDAC1 and oligomeric Aβ (merged **C**) at 100× original magnification.

phosphorylated tau immunoreactivity, indicating that VDAC1 interacts with phosphorylated tau. These results agreed with our immunoprecipitation findings of VDAC1 and phosphorylated tau (Fig. 5). Interestingly, we found not all VDAC1 immunoreactive neurons were positive with the phosphorylated tau antibody, indicating that VDAC1 selectively interacted with phosphorylated tau-positive neurons in the 3XTg.AD mice.

Time-course analysis of mitochondrial dysfunction in APP mice

To determine whether mutant APP and Aβ affect mitochondrial function in APP transgenic mice, we characterized mitochondrial function by measuring H_2O_2 production, cytochrome oxidase activity, lipid peroxidation and ATP production in cerebral cortex tissues from 6-, 12- and 24-month-old APP mice and age-matched non-transgenic WT mice.

H_2O_2 production

We found significantly increased levels of H_2O_2 in the cerebral cortex tissues from 6-month-old ($P = 0.01$), 12-month-old ($P = 0.002$) and 24-month-old ($P = 0.002$) APP mice, relative to the 6-, 12- and 24-month-old WT mice (Fig. 10). To determine whether aging plays a role in altering H_2O_2 production, we also compared the H_2O_2 production data from the 6-month-old WT mice with the data from the 12- and 24-month-old WT mice, and the H_2O_2 production data from the 6-month-old APP mice with the data from the 12- and 24-month-old APP mice. As shown in Figure 10, we found

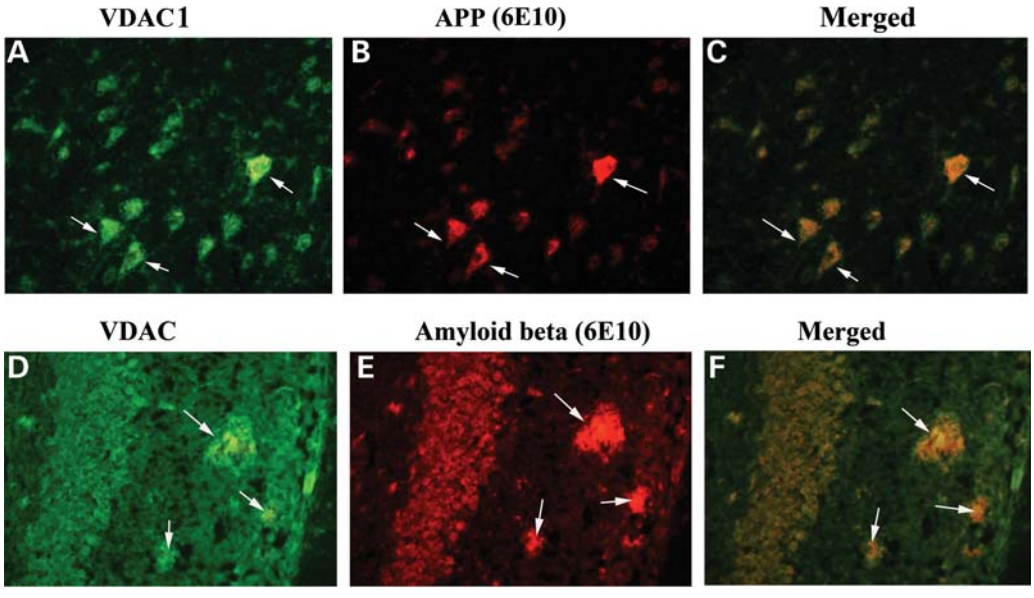

Figure 8. Double-labeling immunofluorescence analysis of VDAC1, Aβ and full-length APP in cortical sections from 20-month-old APP mouse. The localization of VDAC1 (**A**) and APP (**B**) and the colocalization of VDAC1 and APP (merged **C**) at 40× original magnification; the localization of VDAC1 (**D**); Aβ deposits (**E**); and the colocalization of VDAC1 and Aβ deposits (merged **F**) at 100× original magnification, in hippocampal sections from 20-month-old APP mice.

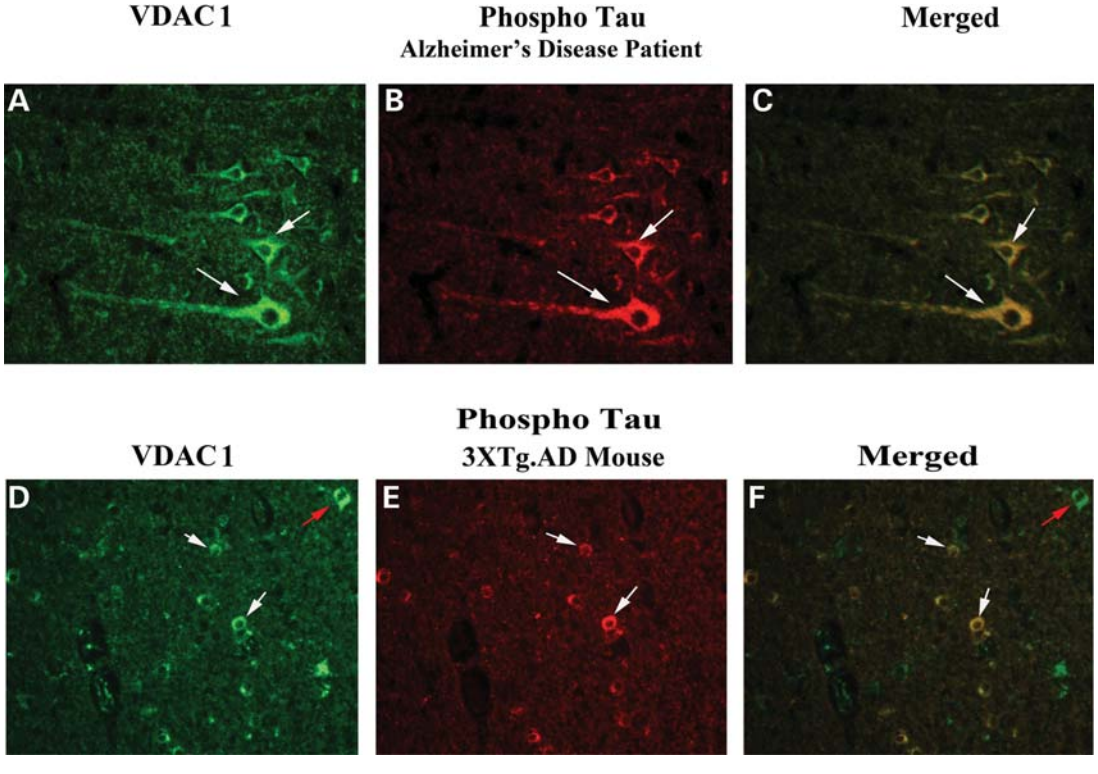

Figure 9. Double-labeling immunofluorescence analysis of VDAC1 and phosphorylated tau in cortical sections from AD patients. The localization of VDAC1 (**A**) and phosphorylated tau (**B**) and the colocalization of VDAC1 and phosphorylated tau (merged **C**) at 40× original magnification; the localization of VDAC1 (**D**) and phosphorylated tau (**E**) and the colocalization of VDAC1 and (merged **F**) at 40× original magnification in cortical sections from 13-month-old APP mouse. White arrows indicate colocalization, and green arrows indicate VDAC1 localization only.

increased levels of H_2O_2 production in the 12-month-old ($P = 0.5$) and 24-month-old ($P = 0.09$) WT mice, relative to the 6-monh-old WT mice but the increase was not significant. However, increased levels of H_2O_2 production were significant in the 12-month-old ($P = 0.04$) and 24-month-old ($P = 0.01$) APP mice, relative to the H_2O_2 production data from the

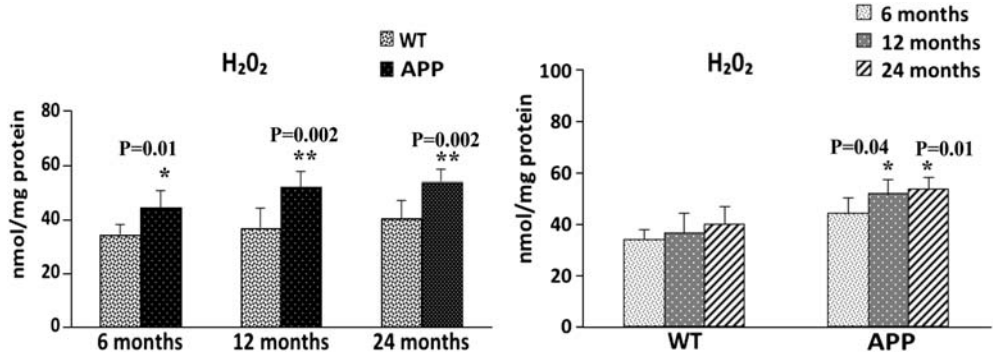

Figure 10. H_2O_2 in cortical mitochondria isolated from 6-, 12- and 24-month-old APP mice and age-matched non-transgenic WT mice. Significantly increased production of H_2O_2 was found in the cerebral cortex from the 6-month-old ($P = 0.01$), 12-month-old ($P = 0.002$) and 24-month-old ($P = 0.002$) APP mice, compared with the 6-, 12- and 24-month-old non-transgenic WT mice. Significantly increased H_2O_2 was found in the 12-month-old ($P = 0.04$) and 24-month-old ($P = 0.01$) APP mice, compared with 6-month-old APP mice.

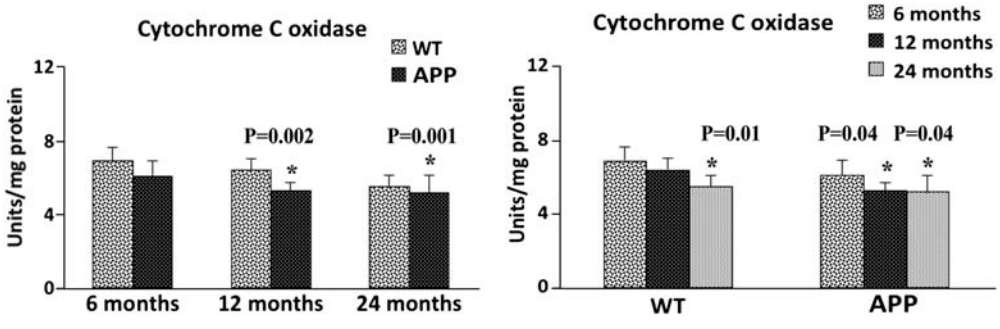

Figure 11. Cytochrome *c* oxidase activity in cortical mitochondria isolated from 6-, 12- and 24-month-old APP mice and age-matched non-transgenic WT mice. Significantly decreased H_2O_2 was found in the cerebral cortex of 12-month-old ($P = 0.002$) and 24-month-old ($P = 0.001$) APP mice, compared with the 12- and 24-month-old non-transgenic WT mice. Significantly reduced H_2O_2 was found in the 12-month-old ($P = 0.04$) and 24-month-old ($P = 0.04$) APP mice, compared with the 6-month-old APP mice.

6-month-old APP mice. These findings suggest both aging and Aβ induce H_2O_2 production, leading to mitochondrial dysfunction in APP mice.

Cytochrome c *oxidase activity*

We found significantly decreased levels of cytochrome oxidase activity in cerebral cortex tissues from the 12-month-old ($P = 0.002$) and 24-month-old ($P = 0.001$) APP mice, relative to the 12- and 24-month-old non-transgenic WT mice (Fig. 11). In the 6-month-old APP mice, cytochrome oxidase levels were decreased, relative to the levels in the age-matched WT mice ($P = 0.17$), but the decrease was not significant. To determine whether aging affects cytochrome oxidase activity, we also compared cytochrome oxidase activity levels of 6- and 12-month-old WT mice with 6- and 12-month-old APP mice. As shown in Figure 11, we found significantly decreased levels of cytochrome oxidase activity in the 12-month-old ($P = 0.002$) and 24-month-old ($P = 0.001$) WT mice, relative to the 6-month-old WT mice. As shown in Figure 11, significantly decreased levels of cytochrome oxidase activity were found in the 12-month-old ($P = 0.04$) and 24-month-old ($P = 0.04$) APP mice, relative to the 6-month-old APP mice. These findings suggest that both aging and Aβ lower cytochrome oxidase activity, leading to mitochondrial dysfunction in APP mice.

Lipid peroxidation

We found significantly increased levels of 4-hydroxy-nonenol (a marker for lipid peroxidation) in cerebral cortex tissues from the 12-month-old ($P = 0.03$) and 24-month-old ($P = 0.01$) APP mice, relative to the 6-, 12- and 24-month-old non-transgenic WT mice (Fig. 12). Increased levels of 4-hydroxy-nonenol were found in the 6-month-old APP mice, but the increase was not significant. To determine whether aging affects lipid peroxidation, we also compared the data of 4-hydroxy-nonenol in 6-, 12- and 24-month-old WT and APP mice. As shown in Figure 12, we found significantly increased levels of 4-hydroxy-nonenol in the 24-month-old APP mice ($P = 0.04$), relative to 6-month-old WT mice. However, significantly increased levels of 4-hydroxy-nonenol were found in 12-month-old ($P = 0.04$) and 24-month-old ($P = 0.002$) APP mice, relative to the 6-month-old APP mice. These observations indicate that both aging and Aβ elevate peroxidation in APP mice.

ATP production

Significantly decreased levels of ATP production were found in the cerebral cortex tissues from the 6-month-old ($P = 0.01$), 12-month-old ($P = 0.003$) and 24-month-old ($P = 0.01$) APP mice, relative to the 6-, 12- and 24-month-old non-transgenic WT mice (Fig. 13). To determine whether aging

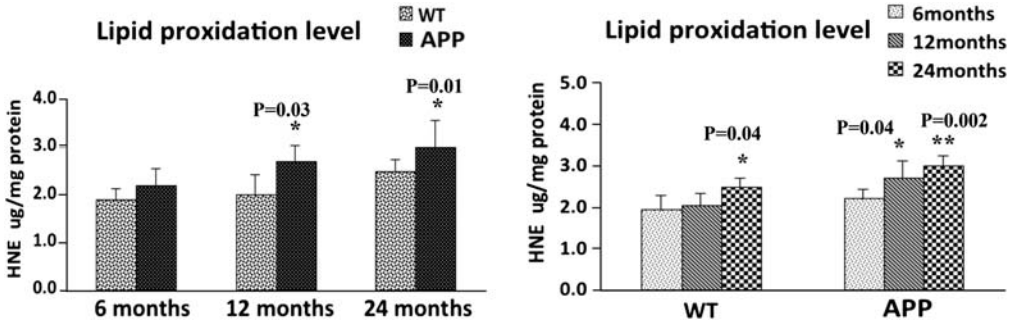

Figure 12. Lipid peroxidation levels in cortical tissues from 6-, 12- and 24-month-old APP mice and age-matched non-transgenic WT mice. Significantly increased 4-hydroxy-nonenol (a marker for lipid peroxidation) levels were found in the cerebral cortex of 12-month-old ($P = 0.03$) and 24-month-old ($P = 0.01$) APP mice, compared with the 12- and 24-month-old non-transgenic WT mice. Significantly increased 4-hydroxy-nonenol levels were found in the 12-month-old ($P = 0.04$) and 24-month-old ($P = 0.02$) APP mice, compared with the 6-month-old APP mice.

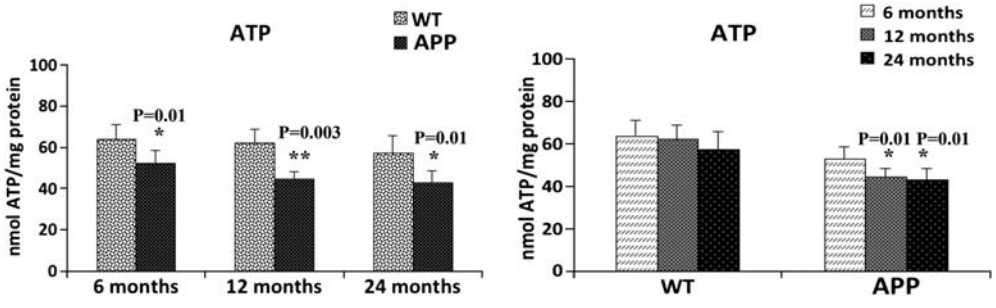

Figure 13. ATP production in cerebral cortical tissues from 6-, 12- and 24-month-old APP mice and age-matched non-transgenic WT mice. Significantly decreased ATP production was found in the cerebral cortex from the 6-month-old ($P = 0.01$), 12-month-old ($P = 0.003$) and 24-month-old ($P = 0.01$) APP mice, compared with the 12- and 24-month-old non-transgenic WT mice. Significantly reduced ATP production was found in the 12-month-old ($P = 0.01$) and 24-month-old ($P = 0.01$) APP mice, compared with the 6-month-old APP mice.

affects ATP production, we also compared ATP levels among the 6-, 12- and 24-month-old WT mice, and also among the 6-, 12- and 24-month-old APP mice. As shown in Figure 13, we found decreased levels of ATP levels in the 12- and 24-month-old WT mice, relative to the 6-month-old WT mice, but the decrease was not significant. As shown in Figure 13, significantly decreased levels of ATP were found in the 12-month-old ($P = 0.01$) and 24-month-old ($P = 0.01$) APP mice, relative to the 6-month-old APP mice.

Fission-induced GTPase activity

We found significantly increased levels of GTPase activity in cerebral cortex tissues from the 12-month-old ($P = 0.002$) and 24-month-old ($P = 0.001$) APP mice, relative to the 12- and 24-month-old non-transgenic WT mice (Fig. 14). Increased levels of GTPase activity were found in the 6-month-old APP mice relative to the age-matched WT mice, but the increase was not significant. To determine whether aging affects GTPase activity, we also compared GTPase activity data in the 6-, 12- and 24-month-old WT mice and APP mice. As shown in Figure 14, significantly increased levels of GTPase activity were found in the 12-month-old ($P = 0.02$) and 24-month-old ($P = 0.01$) APP mice, relative to the 6-month-old APP mice. However, no changes in GTPase activity were found in the 12- and 24-month-old WT mice, relative to the 6-month-old WT mice. These findings suggest that age-dependent increased Aβ levels may enhance fission-linked GTPase activity, leading to mitochondrial fragmentation in APP mice.

DISCUSSION

In the current study, to determine the role of VDAC1 in the progression of AD, we investigated VDAC1 in Braak stages I and II, III and IV, and V and VI of postmortem brains of AD patients and control subjects (Braak stage 0) and 6-, 12- and 24-month-old APP transgenic mice. Further, to determine whether VDAC1 interacts with Aβ (monomers and oligomers) and phosphorylated tau, we studied brains from AD patients and from APP, APP/PS1 and 3XTg.AD mice. To determine whether altered VDAC1 affects mitochondrial function, we also studied mitochondrial function in APP and non-transgenic WT mice. We found progressively increased levels of VDAC1 in the cortical tissues from AD brains relative to control subjects, indicating that VDAC1 is involved in AD progression. Further, we also found significantly increased VDAC1 in the cerebral cortices of 6-, 12- and 24-month-old APP transgenic mice relative to age-matched control WT mice. We also found VDAC1 interacting with Aβ and phosphorylated tau in the brains of AD patients and of APP, APP/PS1 and 3XTg.AD mice. These findings lead us to conclude that VDAC1 interacts with Aβ, and phosphorylated tau may block mitochondrial pores, leading to defects in oxidative phosphorylation and mitochondrial dysfunction in AD pathogenesis.

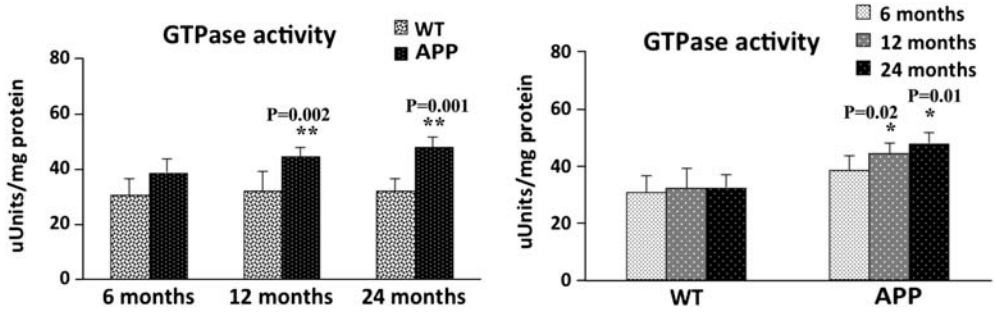

Figure 14. Fission-linked GTPase activity in cortical tissues from 6-, 12- and 24-month-old APP mice and age-matched non-transgenic WT mice. Significantly increased GTPase activity was found in the cerebral cortical tissues from the 12-month-old ($P = 0.002$) and 24-month-old ($P = 0.001$) APP mice, compared with the 12- and 24-month-old non-transgenic WT mice. Significantly increased GTPase activity was found in the 12-month-old ($P = 0.02$) and 24-month-old ($P = 0.01$) APP mice, compared with the 6-month-old APP mice.

Increased VDAC1 in the brains of AD patients and AD mice

VDAC1 is a key regulator of mitochondrial pore opening and pore closure, and it has been used as a housekeeping gene for mitochondrial proteins. VDAC1 is abundantly present in the mitochondrial outer membrane and is highly conserved with structural and electrophysiological features in yeast, plants, mammals, including rodents and humans. Together with mitochondrial inner-membrane proteins, adenine nucleotide transporter (ANT) and CypD, VDAC1 forms a mitochondrial permeability transition (MPT) pore complex. The MPT pore regulation (pore opening and closing) is critical for mitochondrial structure and function. However, in a disease state such as Alzheimer's, Huntington's and other neurodegenerative diseases, mutant proteins are present in the cytoplasm in the vicinity of mitochondria and may interact with VDAC1, likely blocking mitochondrial pores and interrupting the cross-talk between mitochondrial and cytoplasmic/nuclear transport. Further, the protein levels of VDAC1, ANT and CypD need to be balanced to maintain mitochondrial pore opening and closure. However, these proteins are altered in aging and in diseased states. In AD, we (17) and others (38) found increased levels of CypD in brain specimens from AD patients at different stages of disease progression, supporting the possibility that elevated CypD may promote mitochondrial pore opening and may damage the mitochondrial structurally.

To further understand the role of VDAC1 in AD, in the current study, we investigated VDAC1 levels in the brains of AD patients and of 6-, 12- and 24-month-old APP and WT mice. Interestingly, VDAC1 was progressively increased in the AD brains, suggesting that VDAC1 is regulated with disease progression in AD. Further, our comparative analysis of the levels of VDAC1 protein in APP and WT mice revealed that significantly increased levels of VDAC1 in 6-, 12- and 24-month-old APP mice relative to age-matched WT mice, suggesting that mutant APP/or Aβ may be responsible for the increased VDAC1 in APP mice. In addition, our time-course immunoblotting analysis of WT mice found VDAC1 levels to be significantly increased in the 12- and 24-month-old WT mice relative to the 6-month-old WT mice, indicating that VDAC1 increases with age. Overall, these observations indicate that the increase of VDAC1 may be physiologically involved with disease progression in AD by interrupting mitochondrial pore opening and closure.

VDAC1 interacts with Aβ and phosphorylated tau

Our study demonstrated, for the first time, that VDAC1 interacts with: (i) Aβ and full-length APP in AD neurons (Fig. 4A) and (ii) oligomeric Aβ in AD neurons (Fig. 4B). These novel findings suggest that Aβ interacts with VDAC1 and likely forms a VDAC1–Aβ complex in AD neurons. These results complement previously reported Aβ interactions with mitochondrial matrix proteins, alcohol-induced ABAD (21) and CypD (38) in AD neurons.

Aβ may disrupt mitochondrial function in AD neurons in multiple ways. (i) First, by blocking the MPT pores after interacting with VDAC1, which would disrupt the transport of mitochondrial proteins from the nucleus and metabolites, such as ADP and inorganic phosphates. The transport of proteins and metabolites is critical to complete oxidative phosphorylation and to produce mitochondrial ATP. Defective oxidative phosphorylation caused due to abnormal transport of proteins and metabolites may likely induce an increase in free radical production and cause mitochondrial dysfunction. (ii) Second, by entering the mitochondrial matrix and interacting with matrix proteins, ABAD and CypD, and the resultant protein complexes, ABAD + Aβ and CypD + Aβ, which may induce increased free radical production and cause mitochondrial dysfunction.

We also found that VDAC1 interacts with APP mainly on the cis-side of VDAC1, that is, on the side of VDAC1 that faces the cytoplasm. Aβ is also mainly present on the cis-side of VDAC1. Our previous digitonin fractionation analysis of mitochondria from APP mice showed higher levels of Aβ in the outer mitochondrial membrane fraction than in the matrix and in the inner mitochondrial membrane fraction (16). Based on these earlier findings, together with our current findings, we propose that VDAC1 may interact with APP and Aβ, consequently blocking the transport of proteins and metabolites from the cytoplasm to mitochondria, promoting defects in oxidative phosphorylation and causing mitochondrial structural and functional abnormalities.

Overall, the abnormal interactions between Aβ and the matrix proteins ABAD and CypD, and Aβ and VDAC cause mitochondrial dysfunction. These interactions are very specific to affected neuronal populations in AD mice and AD brains, and lead to neuronal damage and cognitive changes.

Similar to the interaction between VDAC1 and Aβ, we also found an interaction between VDAC1 and phosphorylated tau in the brains of AD patients and 3XTg.AD mice (Fig. 5). VDAC1–phosphorylated tau complexes may likely interrupt axonal transport of mitochondria (25), leading to synaptic deprivation and damage in AD neurons.

The interaction of VDAC1 with mutant proteins is not just confined to AD; such interactions also occur in other neurodegenerative diseases, such as ALS and Huntington's. A recent study of ALS transgenic mice (mutant SOD1 mice) revealed that VDAC1 interacts with SOD1, causing mitochondrial dysfunction in mutant SOD1 mice (67). Further, in Huntington's disease knock-in mice Choo *et al*. (68) reported the presence of mutant huntingtin in an outer mitochondrial fraction, and causing intracellular calcium influx and mitochondrial dysfunction in HD neurons (68). In AD, using proteomic analysis followed by western blotting and immunohistochemical techniques, Cuadrado-Tejedor *et al*. (69) found that VDAC1 is overexpressed in the hippocampus from amyloidogenic AD transgenic mice. Interestingly, they also found Aβ-soluble oligomers were able to induce an upregulation of VDAC1 in a human neuroblastoma cell line, further supporting a correlation between Aβ levels and VDAC1 expression. In hippocampal extracts from transgenic mice, a significant increase in the levels of VDAC1 phosphorylated at an epitope was observed to be susceptible to phosphorylation by glycogen synthase kinase-3β, the activity of which also increased (69). Overall, findings from these studies and our current study indicate that mutant proteins, interacting with VDAC1, may block mitochondrial pores, disrupt the transport of proteins and metabolites and cause defects in oxidative phosphorylation, leading to mitochondrial dysfunction and, ultimately, to neuronal damage.

Regarding interaction between Aβ and VDAC1, the C-terminus of the Aβ peptide motif 'GSNKG' (at positions 25–29) has been proposed to interact with the N-terminal motif of VDAC1 'GYGFG' (70). It is possible that the C-terminal motif of Aβ ('GSNKG') could interact with the N-terminal motif of VDAC1 ('GYGFG') since in the current study, we found that VDAC1 interacts with Aβ, and APP in AD neurons. However, further research is needed to identify these proposed 'GXXXG' motif interactions between Aβ and VDAC1 and phosphorylated tau and VDAC1.

Aβ- and phosphorylated tau-induced mitochondrial dysfunction in AD

Oxidative stress and mitochondrial dysfunction have been described in AD pathogenesis. However, what causes oxidative stress and mitochondrial dysfunction in AD are not well understood. Recent studies from our laboratory (16,17,26,71) and others (10,18–20,37) found Aβ interacts with mitochondria, and this abnormal Aβ-mitochondrial interaction may lead to mitochondrial dysfunction. Lustbader *et al*. (21) and Du *et al.* (38) reported Aβ interacting with the mitochondrial matrix proteins, ABAD and CypD, inducing increased free radical production, leading to mitochondrial dysfunction in AD. Hansen Petersen *et al*. (37) reported Aβ-link with inner mitochondrial membrane, and proposed that Aβ-inner membrane may be responsible for oxidative phosphorylation defects. As described earlier, in the current study, we found outer mitochondrial membrane protein, VDAC1 interaction with Aβ, APP and phosphorylated tau, leading to blocking the pores of mitochondria, and mitochondrial transport in AD neurons. Further, we also found defective mitochondrial function (increased levels of H_2O_2 production, lipid peroxidation and mitochondrial fission-linked GTPase activity and reduced cytochrome oxidase activity and mitochondrial ATP) in APP mice. Overall, these time-course analyses of mitochondrial functional parameters in APP mice clearly suggest that mutant APP/Aβ are responsible for a progressive mitochondrial dysfunction in AD.

There are several possible factors that may be responsible for the progressive loss of mitochondrial function in APP mice: (i) progressive increase of VDAC1 in AD neurons, (ii) increasing interaction between VDAC1 and APP/Aβ and phosphorylated tau in AD neurons, resulting in the blockage of mitochondrial pores and leading to defects in oxidative phosphorylation, and (iii) the interaction of Aβ with the matrix proteins ABAD and CypD (21,38). As discussed earlier, for normal mitochondrial function, mitochondrial pores should be controlled and regulated properly. Abnormalities in mitochondrial pore opening and closure may lead to defects in oxidative phosphorylation, mitochondrial dysfunction and ultimately cell death. There are several key mitochondrial proteins, including outer-membrane protein VDAC1, inner-membrane protein ANT and matrix protein CypD, that are involved in mitochondrial pore opening and pore closure. In the current study, we found progressive increased levels of VDAC1, in addition to the previously reported increased levels of CypD (17,38). These elevated levels of VDAC1 and its further interaction with APP, Aβ and phosphorylated tau are responsible for mitochondrial pore blockade and further damage of mitochondria in AD neurons. Based on current study observation, we propose that reduced levels of VDAC1, APP, Aβ and phosphorylated tau may lead to decreased interaction between VDAC1 and APP, Aβ and phosphorylated tau, and may allow mitochondrial pore opening and pore closure, ultimately leading to normal mitochondrial function and ATP supply to nerve terminals and boosting synaptic and cognitive function in AD.

MATERIALS AND METHODS

Postmortem brain sections from AD patients

Twenty postmortem brain specimens from AD patients and age-matched control subjects were obtained from the Harvard Tissue Resource Center, as described previously (17). Fifteen specimens were from patients diagnosed with AD at different stages of disease progression, according to Braak stages 1 and II (early AD) ($n = 5$), III and IV (definite AD) ($n = 5$), V and VI (severe AD) ($n = 5$) (72) and five were from age-matched control subjects. The specimens were from the frontal cortex and were both quick-frozen and formalin-fixed (BA9).

APP, APP/PS1 and 3XTg.AD transgenic mice

Using APP (Tg2576 line) (73), APP/PS1 (74) and 3XTg.AD mice (75) and age-matched WT littermates (controls), we studied the levels of VDAC1 and the relationship of VDAC1 to hyperphosphorylated tau and Aβ at different stages of AD progression. The transgenic Tg2576, APP/PS1 and 3XTg.AD mice were housed at the Oregon National Primate Research Center at Oregon Health & Science University (OHSU). The OHSU Institutional Animal Care and Use Committee approved all procedures for animal care, according to guidelines set forth by the National Institutes of Health.

Antibodies used in this study

To characterize the interaction of VDAC1 with Aβ and with phosphorylated tau, we used an anti-VDAC1 antibody, and antibodies that recognize Aβ peptide monomeric (6E10) and oligomeric (A11) (Invitrogen, CA, USA) and anti-normal tau and anti-phosphorylated tau antibodies. The 6E10 antibody (Covance, Emeryville, CA, USA) was raised against three to eight amino acid residues of a human Aβ peptide. This antibody reacts with a 4 kDa Aβ, derivatives of AβPP and full-length APP. The normal tau antibody that we used was raised against 159–163 amino acid residues of human tau. This antibody recognizes normal tau from humans and bovine. We also used a phosphorylated tau antibody that was raised against a phosphorylated serine 202 and threonine 205 amino acid residues of human tau (Pierce Biotechnology, Inc.). This latter phosphorylated tau antibody recognizes a phosphatase-sensitive epitope on PHF-tau. We also used a phosphorylated tau antibody (PHF-Tau, S396, Abcam, Cambridge, MA, USA) for immunoprecipitation analysis; this antibody was raised a phosphorylated serine, 396 amino acid of human tau.

Immunoblotting analysis of VDAC1 protein

We performed immunoblotting analysis of VDAC1, using lysates from AD postmortem brains (Braak stages I and II, $n = 5$; III and IV, $n = 5$; and V and VI, $n = 5$) and control subjects ($n = 5$) and 6-month-old ($n = 5$), 12-month-old ($n = 5$) and 24-month-old Tg2576 mice and 24-month-old non-transgenic WT mice. Twenty micrograms of protein lysates were resolved on a 4–12% Nu-PAGE gel (Invitrogen, Grand Island, NY, USA). These resolved proteins were transferred to PVDF membranes (Novax, Inc., San Diego, CA, USA) and then incubated with a blocking buffer (5% dry milk dissolved in a TBST buffer) for 1 h at room temperature. The membranes were incubated overnight with primary VDAC1 antibodies (1:200 rabbit polyclonal, Abcam) and β-actin (1:500 mouse monoclonal, Chemicon, Millipore with Sigma-Aldrich, St Louis, MO, USA). The membranes were washed with a TBST buffer three times at 10 min intervals and then incubated for 2 h with an appropriate secondary antibody, followed by three additional washes at 10 min intervals. VDAC1 and beta-actin proteins were detected with a Supersignal West Pico chemiluminescent reagent (Thermo Scientific). Scanned images of the exposed X-ray film were analyzed with ImageJ to determine relative band intensity. Quantification was performed on western blots of cerebral cortex protein lysates from AD postmortem brains and control subjects, and from 6-, 12- and 24-month-old Tg2576 mice and 6-, 12- and 24-month-old non-transgenic WT mice.

Co-immunoprecipitation of VDAC1, Aβ, VDAC1 and phosphorylated tau

To determine whether VDAC1 interacts with Aβ monomers, Aβ oligomers and full-length APP, we used cortical protein lysates from Tg2576 mice, AD patients and control subjects. We performed co-immunoprecipitation assays using a Dynabeads Kit for Immunoprecipitation (Invitrogen). Briefly, 50 μl of Dynabead-containing protein G was incubated with 10 μg of anti-VDAC1 and 6E10 antibodies, for 1 h at room temperature, with rotation. We used all the reagents and buffers that are provided in the kit. Details of antibodies that are used for co-immunoprecipitation and western blotting are given Table 1. The Dynabeads were then washed once with a washing buffer and incubated with rotation overnight, with 500 μg of lysate protein at 4°C. The incubated Dynabead–antigen/antibody complexes were washed again three times with a washing buffer, and an immunoprecipitant was eluted from the Dynabeads, using the NuPAGE LDS sample buffer. The VDAC1 immunoprecipitation elute was loaded onto a 4–20 gradient gel, followed by western blot analysis of VDAC1, 6E10 (monomeric Aβ and full-length APP), oligomeric-specific A11 antibodies.

To determine the interaction between VDAC1 and phosphorylated tau, we performed co-immunoprecipitation analysis using cortical protein lysates from brains of AD patients, control subjects and 20-month-old 3XTg.AD mice, as described earlier. We also cross-checked the results by performing co-immunoprecipitation experiments, using both anti-VDAC1 and anti-phosphorylated tau antibodies, and we conducted western blot analysis, using: (i) VDAC1 immunoprecipitation elutes and a phosphorylated tau antibody and (ii) phosphorylated tau immunoprecipitation elutes and a VDAC1 antibody.

Immunohistochemistry and immunofluorescence analyses

Using immunofluorescence techniques, we studied localization of VDAC1, Aβ and phosphorylated tau in frontal cortex specimens taken from the postmortem brains of the AD patients (17). Briefly, the brain specimens were paraffin-embedded, and sections were cut into widths of 15 μm. We deparaffinized the sections by washing them with xylene for 10 min and then washing them for 5 min in a serial dilution of alcohol (95, 70 and 50%). The sections were then washed once again for 10 min with double-distilled H_2O, and then for six more times at 5 min each, with phosphate-buffered saline (PBS) (pH 7.4). To reduce the autofluorescence of brain specimens, we treated the deparaffinized sections with sodium borohydrate twice each for 30 min, in a freshly prepared 0.1% sodium borohydrate solution dissolved in PBS (pH 8.0). We then washed the sections three times for 5 min each, with PBS (pH 7.4). The brain sections were treated with 0.5% Triton dissolved in PBS (pH 7.4) to increase the antibody permeability. To block the endogenous peroxidase,

Table 2. Summary of antibody dilutions and conditions used in the immunohistochemistry/immunofluorescence analysis in human and mouse

Marker	Primary antibody (species and dilution)	Purchased from (company, state)	Secondary antibody, dilution, Alexa fluor dye	Purchased from (company, city and state)
VDAC	Rabbit polyclonal, 1:200	Abcam, Cambridge, MA	Goat anti-rabbit, biotin 1:300, HRP-streptavidin (1:100), TSA-Alexa488	KPL, Gaithersburg, MD; Vector Laboratories, Inc., Burlingame, CA; Molecular Probe, Eugene, OR
VDAC	Mouse monoclonal, 1:100	MitoSciences, Abcam Cambridge, MA	Goat anti-mouse, biotin 1:300, HRP-streptavidin (1:100), TSA-Alexa594	KPL, Gaithersburg, MD; Vector Laboratories, Inc., Burlingame, CA; Molecular Probe, Eugene, OR
phTau	Mouse monoclonal, 1:100	Pierce Biotechnology, Inc., Rockford, IL	Goat anti-mouse, biotin 1:300, HRP-streptavidin (1:100), TSA-Alexa594	KPL, Gaithersburg, MD; Vector Laboratories, Inc., Burlingame, CA; Molecular Probe, Eugene, OR
6E10	Mouse monoclonal, 1:300	Covance, San Diego, CA	Goat anti-mouse, biotin 1:300, HRP-streptavidin (1:100), TSA-Alexa594	KPL, Gaithersburg, MD; Vector Laboratories, Inc., Burlingame, CA; Molecular Probe, Eugene, OR
A11	Rabbit polyclonal, 1:400	Invitrogen, Camarillo, CA	Goat anti-rabbit, biotin 1:300, HRP-streptavidin (1:100), TSA-Alexa488	KPL, Gaithersburg, MD; Vector Laboratories, Inc., Burlingame, CA; Molecular Probe, Eugene, OR

sections were treated for 15 min with 3% H_2O_2. The sections were blocked for 1 h with a solution of 0.5% Triton in PBS + 10% goat serum + 1% bovine serum albumin. The sections were incubated overnight at room temperature with the following antibodies: anti-VDAC1 (rabbit polyclonal 1:200 dilution, Abcam), Abeta-6E10 antibody (mouse monoclonal, 1:300 dilution, Covance, San Diego, CA, USA) and anti-phosphorylated tau antibody (1:100, mouse monoclonal; Pierce Biotechnology, Inc.). On the day after the primary antibody incubation, sections were washed once with 0.1% Triton in PBS and then incubated with appropriate biotinylated secondary antibodies for 1 h at room temperature. Details of the secondary antibodies are given in Table 2. They were washed with PBS three times for 10 min each and then incubated for 1 h with a horseradish peroxidase (HRP)-conjugated streptavidin solution (Invitrogen). The sections were each washed three more times with PBS (pH 7.4) for 10 min each and then treated with Tyramide Alexa 594 (red) or Alexa 488 (green) (Molecular Probes, Eugene, OR, USA) for 10 min at room temperature. They were cover-slipped with Prolong Gold and photographed with a confocal microscope.

Double-labeling immunofluorescence analysis

To determine the interaction between VDAC1 and phosphorylated tau, and VDAC1 and Aβ (monomers and oligomers and full-length APP), we conducted double-labeling immunofluorescence analysis, using an anti-VDAC1 antibody, an anti-phosphorylated tau antibody and VDAC1, 6E10 and A11 antibodies. As described earlier, postmortem brain sections from patients with AD and control subjects were deparaffinized and treated with sodium borohydrate to reduce autofluorescence. For the first labeling, the sections were incubated overnight with appropriate primary antibodies at room temperature. On the day after this incubation, the sections were washed with 0.5% Triton in PBS and then incubated with a secondary biotinylated anti-rabbit antibody, at a 1:300 dilution (Vector Laboratories, Burlingame, CA, USA), or with a secondary biotinylated anti-mouse antibody (1:300) for 1 h at room temperature. Details of primary and secondary antibodies are given in Table 2. The antibodies were incubated for 1 h in an HRP-conjugated streptavidin solution (Molecular Probes). The sections were then washed three times with PBS, each for 10 min at pH 7.4. They were then treated with Tyramide Alexa488 for 10 min at room temperature. For the second labeling, the sections were incubated overnight with an anti-phosphorylated tau antibody (1:100, mouse monoclonal; Pierce Biotechnology, Inc.) at room temperature. They were incubated with a donkey, anti-mouse secondary antibody that was labeled with Alexa 594 for 1 h at room temperature. The sections were cover-slipped with Prolong Gold and photographed with a confocal microscope.

We also performed double-labeling analyses of VDAC1 and phospho tau, and VDAC1, Aβ and full-length APP, using midbrain sections from Tg2576 mice and 3XTg.AD mice and VDAC1 and phosphorylated tau, and VDAC1 and Aβ (monomers and oligomers) and full-length APP, as described earlier.

Mitochondrial dysfunction in WT and APP mice

Using cerebral cortex tissues from 6-, 12- and 24-month-old Tg2576 and age-matched non-transgenic WT mice (five mice for each time point for both Tg2576 and WT mice), we measured mitochondrial functional parameters, including H_2O_2 production, cytochrome oxidase activity, 4-hydroxy-2-nonenol (HNE) levels (lipid peroxidation), ATP production and fission-linked GTPase activity.

H_2O_2 production

Using an Amplex® Red H_2O_2 Assay Kit (Molecular Probes), we measured the production of H_2O_2 in the tissues from the cerebral cortex, as previously described in Manczak *et al.* (76). Briefly, H_2O_2 was measured in mitochondria isolated from the cerebral cortex tissues. A BCA Protein Assay Kit (Pierce Biotechnology) was used to measure protein concentration in a reaction mixture that contained mitochondrial proteins (μg/μl), Amplex red reagents (50 μM), HRP (0.1 U/ml) and a reaction buffer (1×). The mixture was incubated at room temperature for 30 min, followed by spectrophotometer readings of fluorescence (570 nm). Finally, H_2O_2 production was determined using a standard curve equation expressed in nmol/μg mitochondrial protein.

Cytochrome oxidase activity

Cytochrome oxidase activity was measured in mitochondria isolated from cerebral cortex tissues, as described in Manczak *et al.* (76). Enzyme activity was assayed spectrophotometrically with a Sigma Kit (Sigma-Aldrich) following the manufacturer's instructions. Briefly, 2 μg of mitochondrial protein was added to 1.1 ml of a reaction solution containing 50 μl of 0.22 mM ferricytochrome *c* fully reduced by DTT, Tris–HCl at pH 7.0 and 120 mM potassium chloride. The absorbance of wavelength at 550 nm was recorded in 1 min reactions, at 10 s intervals. Cytochrome *c* oxidase activity was measured according to the following formula: mU/mg total mitochondrial protein = (A/min sample − (A/min blank) × 1.1 ml × 21.84). The protein concentrations were determined following the BCA method.

ATP levels

The levels of ATP were measured in mitochondria from cerebral cortex tissues, with an ATP determination kit (Molecular Probes). This bioluminescence assay is based on the reaction of ATP with recombinant firefly luciferase and its substract luciferin. Luciferase catalyzes the formation of light from ATP and luciferin. The emitted light is linearly related to the concentration of ATP, which is measured using a luminometer. We measured ATP from mitochondrial pellets, using a standard curve method.

Lipid peroxidation assay

Lipid peroxidates are unstable indicators of oxidative stress in neurons. HNE is the final product of lipid peroxidation that can be measured in cerebral cortex tissues, with an HNE-His ELISA Kit (Cell BioLabs, Inc., San Diego, CA, USA). In our study, freshly prepared protein lysates were added to a 96-well protein-binding plate and incubated overnight at 4°C. It was then washed three times with a wash buffer. The anti-HNE-His antibody was then added to wells and incubated for 2 h at room temperature, and then was washed three times. Next, the samples were incubated with a secondary antibody that was conjugated with peroxidase for 2 h at room temperature. The samples were then incubated with an enzyme substrate. Optical density was measured to quantify the level of HNE (lipid peroxidation).

GTPase enzymatic activity

Using a Novus Biologicals calorimetric kit (Littleton, CO, USA), we measured GTPase enzymatic activity in cerebral cortex tissues, following GTPase assay methods described in Shirendeb *et al.* (77), based on GTP hydrolyzing to GDP and to inorganic Pi. We measured GTPase activity, based on the amount of Pi that the GTP produces. By adding the ColorLock Gold (orange) substrate to the Pi generated from GTP, we assessed GTP activity, based on the inorganic complex solution (green). Colorimetric measurements (green) were read in the wavelength range of 650 nm. We compared GTPase activity in the cerebral cortex tissues from the Tg2576 mice with WT mice and also performed time-course analyses across the Tg2576 mice and across the WT mice.

ACKNOWLEDGEMENTS

We thank Dr Anda Cornia (Imaging Core of the OHSU Oregon National Primate Research Center) for her assistance with the confocal microscopy. We also thank Drs Karen Ashe, David Borchelt, Frank LaFerla and Salvotore Oddo for the generous gifts of APP, APP/PS1 and 3XTg.AD mice.

Conflict of Interest statement. None declared.

FUNDING

This research was supported by NIH grants AG028072, AG042178, RR000163 (P.H.R.), P30-NS061800 (PI, Aicher) and a grant from the Alzheimer Association (IIRG-09–092429, P.H.R.).

REFERENCES

1. Selkoe, D.J. (2001) Alzheimer's disease: genes, proteins, and therapy. *Physiol. Rev.*, **81**, 741–766.
2. Mattson, M.P. (2004) Pathways towards and away from Alzheimer's disease. *Nature*, **430**, 631–639.
3. LaFerla, F.M., Green, K.N. and Oddo, S. (2007) Intracellular amyloid-beta in Alzheimer's disease. *Nat. Rev. Neurosci.*, **8**, 499–509.
4. Reddy, P.H. and Beal, M.F. (2008) Amyloid beta, mitochondrial dysfunction and synaptic damage: implications for cognitive decline in aging and Alzheimer's disease. *Trends Mol. Med.*, **14**, 45–53.
5. Reddy, P.H., Manczak, M., Mao, P., Calkins, M.J., Reddy, A.P. and Shirendeb, U. (2010) Amyloid-beta and mitochondria in aging and Alzheimer's disease: implications for synaptic damage and cognitive decline. *J. Alzheimers Dis.*, **20**, 499–512.
6. Swerdlow, R.H. and Khan, S.M. (2004) A 'mitochondrial cascade hypothesis' for sporadic Alzheimer's disease. *Med. Hypotheses*, **63**, 8–20.
7. Du, H., Guo, L., Yan, S., Sosunov, A.A., McKhann, G.M. and Yan, S.S. (2010) Early deficits in synaptic mitochondria in an Alzheimer's disease mouse model. *Proc. Natl Acad. Sci. USA*, **107**, 18670–18675.
8. Praticò, D., Uryu, K., Leight, S., Trojanoswki, J.Q. and Lee, V.M. (2001) Increased lipid peroxidation precedes amyloid plaque formation in an animal model of Alzheimer amyloidosis. *J. Neurosci.*, **21**, 4183–4187.
9. Manczak, M., Park, B.S., Jung, Y. and Reddy, P.H. (2004) Differential expression of oxidative phosphorylation genes in patients with Alzheimer's disease: implications for early mitochondrial dysfunction and oxidative damage. *Neuromolecular Med.*, **5**, 147–162.
10. Devi, L., Prabhu, B.M., Galati, D.F., Avadhani, N.G. and Anandatheerthavarada, H.K. (2006) Accumulation of amyloid precursor protein in the mitochondrial import channels of human Alzheimer's disease brain is associated with mitochondrial dysfunction. *J. Neurosci.*, **26**, 9057–9068.
11. Hirai, K., Aliev, G., Nunomura, A., Fujioka, H., Russell, R.L., Atwood, C.S., Johnson, A.B., Kress, Y., Vinters, H.V., Tabaton, M. *et al.* (2001) Mitochondrial abnormalities in Alzheimer's disease. *J. Neurosci.*, **21**, 3017–3023.
12. Parker, W.D. Jr., Filley, C.M. and Parks, J.K. (1990) Cytochrome oxidase deficiency in Alzheimer's disease. *Neurology*, **40**, 1302–1303.
13. Maurer, I., Zierz, S. and Möller, H.J. (2000) A selective defect of cytochrome *c* oxidase is present in brain of Alzheimer disease patients. *Neurobiol. Aging*, **21**, 455–462.
14. Smith, M.A., Perry, G., Richey, P.L., Sayre, L.M., Anderson, V.E., Beal, M.F. and Kowall, N. (1996) Oxidative damage in Alzheimer's. *Nature*, **382**, 120–121.
15. Reddy, P.H., McWeeney, S., Park, B.S., Manczak, M., Gutala, R.V., Partovi, D., Jung, Y., Yau, V., Searles, R., Mori, M. and Quinn, J. (2004) Gene expression profiles of transcripts in amyloid precursor protein transgenic mice: up-regulation of mitochondrial metabolism and apoptotic genes is an early cellular change in Alzheimer's disease. *Hum. Mol. Genet.*, **13**, 1225–1240.
16. Manczak, M., Anekonda, T.S., Henson, E., Park, B.S., Quinn, J. and Reddy, P.H. (2006) Mitochondria are a direct site of A beta accumulation

in Alzheimer's disease neurons: implications for free radical generation and oxidative damage in disease progression. *Hum. Mol. Genet.*, **15**, 1437–1449.
17. Manczak, M., Calkins, M.J. and Reddy, P.H. (2011) Impaired mitochondrial dynamics and abnormal interaction of amyloid beta with mitochondrial protein Drp1 in neurons from patients with Alzheimer's disease: implications for neuronal damage. *Hum. Mol. Genet.*, **20**, 2495–2509.
18. Caspersen, C., Wang, N., Yao, J., Sosunov, A., Chen, X., Lustbader, J.W., Xu, H.W., Stern, D., McKhann, G. and Yan, S.D. (2005) Mitochondrial Abeta: a potential focal point for neuronal metabolic dysfunction in Alzheimer's disease. *FASEB J.*, **19**, 2040–2041.
19. Yao, J., Irwin, R.W., Zhao, L., Nilsen, J., Hamilton, R.T. and Brinton, R.D. (2009) Mitochondrial bioenergetic deficit precedes Alzheimer's pathology in female mouse model of Alzheimer's disease. *Proc. Natl Acad. Sci. USA*, **106**, 14670–14675.
20. Devi, L. and Ohno, M. (2012) Mitochondrial dysfunction and accumulation of the β-secretase-cleaved C-terminal fragment of APP in Alzheimer's disease transgenic mice. *Neurobiol. Dis.*, **45**, 417–424.
21. Lustbader, J.W., Cirilli, M., Lin, C., Xu, H.W., Takuma, K., Wang, N., Caspersen, C., Chen, X., Pollak, S., Chaney, M. *et al.* (2004) ABAD directly links Abeta to mitochondrial toxicity in Alzheimer's disease. *Science*, **304**, 448–452.
22. Li, F., Calingasan, N.Y., Yu, F., Mauck, W.M., Toidze, M., Almeida, C.G., Takahashi, R.H., Carlson, G.A., Beal, M.F., Lin, M.T. and Gouras, G.K. (2004) Increased plaque burden in brains of APP mutant MnSOD heterozygous knockout mice. *J. Neurochem.*, **89**, 1308–1312.
23. Eckert, A., Hauptmann, S., Scherping, I., Rhein, V., Muller-Spahn, F., Götz, J. and Muller, W.E. (2008) Soluble beta amyloid leads to mitochondrial defects in amyloid precursor protein and tau transgenic mice. *Neurodegener. Dis.*, **5**, 157–159.
24. Calkins, M.J. and Reddy, P.H. (2011) Amyloid beta impairs mitochondrial anterograde transport and degenerates synapses in Alzheimer's disease neurons. *Biochim. Biophys. Acta*, **1812**, 507–513.
25. Calkins, M.J., Manczak, M., Mao, P., Shirendeb, U. and Reddy, P.H. (2011) Impaired mitochondrial biogenesis, defective axonal transport of mitochondria, abnormal mitochondrial dynamics and synaptic degeneration in a mouse model of Alzheimer's disease. *Hum. Mol. Genet.*, **20**, 4515–4529.
26. Manczak, M., Mao, P., Calkins, M.J., Cornea, A., Reddy, A.P., Murphy, M.P., Szeto, H.H., Park, B. and Reddy, P.H. (2010) Mitochondria-targeted antioxidants protect against amyloid-beta toxicity in Alzheimer's disease neurons. *J. Alzheimers Dis.*, **20**, 609–631.
27. Wang, X., Su, B., Siedlak, S.L., Moreira, P.I., Fujioka, H., Wang, Y., Casadesus, G. and Zhu, X. (2008) Amyloid-beta overproduction causes abnormal mitochondrial dynamics via differential modulation of mitochondrial fission/fusion proteins. *Proc. Natl Acad. Sci. USA*, **105**, 19318–19323.
28. Wang, X., Su, B., Lee, H.G., Li, X., Perry, G., Smith, M.A. and Zhu, X. (2009) Impaired balance of mitochondrial fission and fusion in Alzheimer's disease. *J. Neurosci.*, **29**, 9090–9103.
29. Wang, X., Perry, G., Smith, M.A. and Zhu, X. (2010) Amyloid-beta-derived diffusible ligands cause impaired axonal transport of mitochondria in neurons. *Neurodegener. Dis.*, **7**, 56–59.
30. Diana, A., Simić, G., Sinforiani, E., Orrù, N., Pichiri, G. and Bono, G. (2008) Mitochondria morphology and DNA content upon sublethal exposure to beta-amyloid(1-42) peptide. *Coll. Antropol.*, **32**, 51–58.
31. Schmidt, C., Lepsverdize, E., Chi, S.L., Das, A.M., Pizzo, S.V., Dityatev, A. and Schachner, M. (2008) Amyloid precursor protein and amyloid beta-peptide bind to ATP synthase and regulate its activity at the surface of neural cells. *Mol. Psychiatry*, **13**, 953–969.
32. Matsumoto, K., Akao, Y., Yi, H., Shamoto-Nagai, M., Maruyama, W. and Naoi, M. (2006) Overexpression of amyloid precursor protein induces susceptibility to oxidative stress in human neuroblastoma SH-SY5Y cells. *J. Neural. Transm.*, **113**, 125–135.
33. Gibson, G.E., Sheu, K.F. and Blass, J.P. (1998) Abnormalities of mitochondrial enzymes in Alzheimer disease. *J. Neural. Transm.*, **105**, 855–870.
34. Wang, J., Xiong, S., Xie, C., Markesbery, W.R. and Lovell, M.A. (2005) Increased oxidative damage in nuclear and mitochondrial DNA in Alzheimer's disease. *J. Neurochem.*, **93**, 953–962.
35. Sultana, R., Boyd-Kimball, D., Cai, J., Pierce, W.M., Klein, J.B., Merchant, M. and Butterfield, D.A. (2007) Proteomics analysis of the Alzheimer's disease hippocampal proteome. *J. Alzheimers Dis.*, **11**, 153–164.
36. Crouch, P.J., Blake, R., Duce, J.A., Ciccotosto, G.D., Li, Q.X., Barnham, K.J., Curtain, C.C., Cherny, R.A., Cappai, R., Dyrks, T., Masters, C.L. and Trounce, I.A. (2005) Copper-dependent inhibition of human cytochrome *c* oxidase by a dimeric conformer of amyloid-beta1-42. *J. Neurosci.*, **25**, 672–679.
37. Hansson Petersen, C.A., Alikhani, N., Behbahani, H., Wiehager, B., Pavlov, P.F., Alafuzoff, I., Leinonen, V., Ito, A., Winblad, B., Glaser, E. and Ankarcrona, M. (2008) The amyloid beta-peptide is imported into mitochondria via the TOM import machinery and localized to mitochondrial cristae. *Proc. Natl Acad. Sci. USA*, **105**, 13145–13150.
38. Du, H., Guo, L., Fang, F., Chen, D., Sosunov, A.A., McKhann, G.M., Yan, Y., Wang, C., Zhang, H., Molkentin, J.D. *et al.* (2008) Cyclophilin D deficiency attenuates mitochondrial and neuronal perturbation and ameliorates learning and memory in Alzheimer's disease. *Nat. Med.*, **14**, 1097–1105.
39. Reddy, P.H. (2011) Abnormal tau, mitochondrial dysfunction, impaired axonal transport of mitochondria, and synaptic deprivation in Alzheimer's disease. *Brain Res.*, **1415**, 136–148.
40. Ebneth, A., Godemann, R., Stamer, K., Illenberger, S., Trinczek, B. and Mandelkow, E. (1998) Overexpression of tau protein inhibits kinesin-dependent trafficking of vesicles, mitochondria, and endoplasmic reticulum: implications for Alzheimer's disease. *J. Cell Biol.*, **143**, 777–794.
41. Stamer, K., Vogel, R., Thies, E., Mandelkow, E. and Mandelkow, E.M. (2002) Tau blocks traffic of organelles, neurofilaments, and APP vesicles in neurons and enhances oxidative stress. *J. Cell Biol.*, **156**, 1051–1063.
42. Mandelkow, E.M., Stamer, K., Vogel, R., Thies, E. and Mandelkow, E. (2003) Clogging of axons by tau, inhibition of axonal traffic and starvation of synapses. *Neurobiol. Aging*, **24**, 1079–1085.
43. Dubey, M., Chaudhury, P., Kabiru, H. and Shea, T.B. (2008) Tau inhibits anterograde axonal transport and perturbs stability in growing axonal neurites in part by displacing kinesin cargo: neurofilaments attenuate tau-mediated neurite instability. *Cell Motil. Cytoskeleton*, **65**, 89–99.
44. Vossel, K.A., Zhang, K., Brodbeck, J., Daub, A.C., Sharma, P., Finkbeiner, S., Cui, B. and Mucke, L. (2010) Tau reduction prevents Abeta-induced defects in axonal transport. *Science*, **330**, 198.
45. Resende, R., Moreira, P.I., Proença, T., Deshpande, A., Busciglio, J., Pereira, C. and Oliveira, C.R. (2008) Brain oxidative stress in a triple-transgenic mouse model of Alzheimer disease. *Free Radic. Biol. Med.*, **44**, 2051–2057.
46. Sensi, S.L., Rapposelli, I.G., Frazzini, V. and Mascetra, N. (2008) Altered oxidant-mediated intraneuronal zinc mobilization in a triple transgenic mouse model of Alzheimer's disease. *Exp. Gerontol.*, **43**, 488–492.
47. David, D.C., Hauptmann, S., Scherping, I., Schuessel, K., Keil, U., Rizzu, P., Ravid, R., Dröse, S., Brandt, U., Muller, W.E., Eckert, A. and Götz, J. (2005) Proteomic and functional analyses reveal a mitochondrial dysfunction in P301L tau transgenic mice. *J. Biol. Chem.*, **280**, 23802–23814.
48. Dumont, M., Stack, C., Elipenahli, C., Jainuddin, S., Gerges, M., Starkova, N.N., Yang, L., Starkov, A.A. and Beal, F. (2011) Behavioral deficit, oxidative stress, and mitochondrial dysfunction precede tau pathology in P301S transgenic mice. *FASEB J.*, **25**, 4063–4072.
49. Rhein, V., Song, X., Wiesner, A., Ittner, L.M., Baysang, G., Meier, F., Ozmen, L., Bluethmann, H., Dröse, S., Brandt, U. *et al.* (2009) Amyloid-beta and tau synergistically impair the oxidative phosphorylation system in triple transgenic Alzheimer's disease mice. *Proc. Natl Acad. Sci. USA*, **106**, 20057–20062.
50. Chou, J.L., Shenoy, D.V., Thomas, N., Choudhary, P.K., Laferla, F.M., Goodman, S.R. and Breen, G. (2011) Early dysregulation of the mitochondrial proteome in a mouse model of Alzheimer's disease. *J. Proteomics*, **74**, 466–479.
51. Reddy, P.H. (2007) Mitochondrial dysfunction in aging and Alzheimer's disease: strategies to protect neurons. *Antioxid. Redox Signal.*, **10**, 1647–1658.
52. Hodge, T. and Colombini, M. (1997) Regulation of metabolite flux through voltage-gating of VDAC channels. *J Membr. Biol.*, **157**, 271–279.
53. Xu, X. and Colombini, M. (1997) Autodirected insertion: preinserted VDAC channels greatly shorten the delay to the insertion of new channels. *Biophys. J.*, **72**, 2129–2136.

54. Rostovtseva, T. and Colombini, M. (1997) VDAC channels mediate and gate the flow of ATP: implications for the regulation of mitochondrial function. *Biophys. J.*, **72**, 1954–1962.
55. Colombini, M. (2012) VDAC structure, selectivity, and dynamics. *Biochim. Biophys. Acta*, **1818**, 1457–1465.
56. Sampson, M.J., Lovell, R.S., Davison, D.B. and Craigen, W.J. (1996) A novel mouse mitochondrial voltage-dependent anion channel gene localizes to chromosome 8. *Genomics*, **36**, 192–196.
57. Sampson, M.J., Lovell, R.S. and Craigen, W.J. (1996) Isolation, characterization, and mapping of two mouse mitochondrial voltage-dependent anion channel isoforms. *Genomics*, **33**, 283–288.
58. Craigen, W.J. and Graham, B.H. (2008) Genetic strategies for dissecting mammalian and *Drosophila* voltage-dependent anion channel functions. *J. Bioenerg. Biomembr.*, **40**, 207–212.
59. Yamamoto, T., Yamada, A., Watanabe, M., Yoshimura, Y., Yamazaki, N., Yoshimura, Y., Yamauchi, T., Kataoka, M., Nagata, T., Terada, H. and Shinohara, Y. (2006) VDAC1, having a shorter N-terminus than VDAC2 but showing the same migration in an SDS-polyacrylamide gel, is the predominant form expressed in mitochondria of various tissues. *J. Proteome Res.*, **5**, 3336–3344.
60. Sampson, M.J., Ross, L., Decker, W.K. and Craigen, W.J. (1998) A novel isoform of the mitochondrial outer membrane protein VDAC3 via alternative splicing of a 3-base exon. Functional characteristics and subcellular localization. *J. Biol. Chem.*, **273**, 30482–30486.
61. Raghavan, A., Sheiko, T., Graham, B.H. and Craigen, W.J. (2012) Voltage-dependant anion channels: novel insights into isoform function through genetic models. *Biochim. Biophys. Acta*, **1818**, 1477–1485.
62. Shimizu, S., Narita, M. and Tsujimoto, Y. (1999) Bcl-2 family proteins regulate the release of apoptogenic cytochrome *c* by the mitochondrial channel VDAC. *Nature*, **399**, 483–487.
63. Zheng, Y., Shi, Y., Tian, C., Jiang, C., Jin, H., Chen, J., Almasan, A., Tang, H. and Chen, Q. (2004) Essential role of the voltage-dependent anion channel (VDAC) in mitochondrial permeability transition pore opening and cytochrome *c* release induced by arsenic trioxide. *Oncogene*, **23**, 1239–1247.
64. Rostovtseva, T.K. and Bezrukov, S.M. (2012) VDAC inhibition by tubulin and its physiological implications. *Biochim. Biophys. Acta*, **1818**, 1526–1535.
65. Kerner, J., Lee, K., Tandler, B. and Hoppel, C.L. (2012) VDAC proteomics: post-translation modifications. *Biochim. Biophys. Acta*, **1818**, 1520–1525.
66. Lemasters, J.J., Holmuhamedov, E.L., Czerny, C., Zhong, Z. and Maldonado, E.N. (2012) Regulation of mitochondrial function by voltage dependent anion channels in ethanol metabolism and the Warburg effect. *Biochim. Biophys. Acta*, **1818**, 1536–1544.
67. Israelson, A., Arbel, N., Da Cruz, S., Ilieva, H., Yamanaka, K., Shoshan-Barmatz, V. and Cleveland, D.W. (2010) Misfolded mutant SOD1 directly inhibits VDAC1 conductance in a mouse model of inherited ALS. *Neuron*, **67**, 575–587.
68. Choo, Y.S., Johnson, G.V., MacDonald, M., Detloff, P.J. and Lesort, M. (2004) Mutant huntingtin directly increases susceptibility of mitochondria to the calcium-induced permeability transition and cytochrome c release. *Hum. Mol. Genet.*, **13**, 1407–1420.
69. Cuadrado-Tejedor, M., Vilariño, M., Cabodevilla, F., Del Río, J., Frechilla, D. and Pérez-Mediavilla, A. (2011) Enhanced expression of the voltage-dependent anion channel 1 (VDAC1) in Alzheimer's disease transgenic mice: an insight into the pathogenic effects of amyloid-β. *J. Alzheimers Dis.*, **23**, 195–206.
70. Thinnes, F.P. (2011) Apoptogenic interactions of plasmalemmal type-1 VDAC and Aβ peptides via GxxxG motifs induce Alzheimer's disease – a basic model of apoptosis? *Wien. Med. Wochenschr.*, **161**, 274–276.
71. Manczak, M. and Reddy, P.H. (2012) Abnormal interaction between the mitochondrial fission protein Drp1 and hyperphosphorylated tau in Alzheimer's disease neurons: implications for mitochondrial dysfunction and neuronal damage. *Hum. Mol. Genet.*, **21**, 2538–2547.
72. Braak, H. and Braak, E. (1991) Demonstration of amyloid deposits and neurofibrillary changes in whole brain sections. *Brain Pathol.*, **1**, 213–216.
73. Hsiao, K., Chapman, P., Nilsen, S., Eckman, C., Harigaya, Y., Younkin, S., Yang, F. and Cole, G. (1996) Correlative memory deficits, Abeta elevation, and amyloid plaques in transgenic mice. *Science*, **274**, 99–102.
74. Borchelt, D.R., Ratovitski, T., van Lare, J., Lee, M.K., Gonzales, V., Jenkins, N.A., Copeland, N.G., Price, D.L. and Sisodia, S.S. (1997) Accelerated amyloid deposition in the brains of transgenic mice coexpressing mutant presenilin 1 and amyloid precursor proteins. *Neuron*, **19**, 939–945.
75. Oddo, S., Caccamo, A., Shepherd, J.D., Murphy, M.P., Golde, T.E., Kayed, R., Metherate, R., Mattson, M.P., Akbari, Y. and LaFerla, F.M. (2003) Triple-transgenic model of Alzheimer's disease with plaques and tangles: intracellular Abeta and synaptic dysfunction. *Neuron*, **39**, 409–421.
76. Manczak, M., Sesaki, H., Kageyama, Y. and Reddy, P.H. (2012) Dynamin-related protein 1 heterozygote knockout mice do not have synaptic and mitochondrial deficiencies. *Biochim. Biophys. Acta*, **1822**, 862–874.
77. Shirendeb, U.P., Calkins, M.J., Manczak, M., Anekonda, V., Dufour, B., McBride, J.L., Mao, P. and Reddy, P.H. (2012) Mutant huntingtin's interaction with mitochondrial protein Drp1 impairs mitochondrial biogenesis and causes defective axonal transport and synaptic degeneration in Huntington's disease. *Hum. Mol. Genet.*, **21**, 406–420.